
Rethinking Value Function Learning for Generalization in Reinforcement Learning

Seungyong Moon^{1,2}, JunYeong Lee^{1,2}, Hyun Oh Song^{1,2,3*}

¹Seoul National University, ²Neural Processing Research Center, ³DeepMetrics
{symoon11, mascheroni99, hyunoh}@ml1ab.snu.ac.kr

Abstract

We focus on the problem of training RL agents on multiple training environments to improve observational generalization performance. In prior methods, policy and value networks are separately optimized using a disjoint network architecture to avoid interference and obtain a more accurate value function. We identify that the value network in the multiple-environment setting is more challenging to optimize and prone to overfitting training data than in the conventional single-environment setting. In addition, we find that appropriate regularization of the value network is required for better training and test performance. To this end, we propose Delayed-Critic Policy Gradient (DCPG), which implicitly penalizes the value estimates by optimizing the value network less frequently with more training data than the policy network, which can be implemented using a shared network architecture. Furthermore, we introduce a simple self-supervised task that learns the forward and inverse dynamics of environments using a single discriminator, which can be jointly optimized with the value network. Our proposed algorithms significantly improve observational generalization performance and sample efficiency in the Progen Benchmark.

1 Introduction

In recent years, deep reinforcement learning (RL) has achieved remarkable success in various domains, such as robotic controls and games [32, 21, 38]. To apply RL algorithms to more practical scenarios, such as autonomous vehicles or healthcare systems, they should be robust against the non-stationarity of real-world environments and capable of performing well on unseen situations during deployment. However, current state-of-the-art RL algorithms often fail to generalize to unseen test environments with visual variation (*i.e.*, observational generalization), even if they achieve high performance in the training environments [16, 46, 9].

Training RL agents on a finite number of environments and testing them on unseen environments is the standard protocol for evaluating observational generalization in RL [10]. Several methods have attempted to improve the generalization in this framework by adopting the regularization techniques that originate from supervised learning or training robust state representations via self-supervised learning [9, 22, 36, 31]. However, these methods have mainly focused on developing new auxiliary objectives on the existing RL algorithms intended for the conventional single-environment setting such as PPO [40]. Some recent works have investigated the interference between policy and value function optimization arising from the multiple training environments and proposed new RL training schemes that decouple the policy and value network training with a separate network architecture to obtain an accurate value function [11, 35].

*Corresponding author

In this paper, we argue that learning an accurate value function in the multi-environment setting is more challenging than in the single-environment setting and should be optimized with sufficient regularization. We identify that the value network trained on multiple environments is more likely to memorize the training data and cannot generalize to unvisited states of the training environments, which acts detrimentally to not only the training performance but also the test performance on unseen environments. In addition, we find that regularization methods that penalize large estimates of the value network, initially developed for preventing overfitting in the single-environment setting, are also beneficial for improving both the training and test performance in the multi-environment setting. However, this benefit comes at the cost of premature convergence, which hinders further performance enhancement.

To this end, we propose a new model-free policy gradient algorithm named *Delayed-Critic Policy Gradient* (DCPG), which trains the value network with less update frequency but with more training data than the policy network. We find that the value network with delayed updates suffers less from the overfitting problem and significantly improves both the training and test performance. In addition, we demonstrate that it provides better representations to the policy network using a single unified network architecture, unlike the prior methods. Moreover, we introduce a simple self-supervised task that learns the forward and inverse dynamics of environments using a single discriminator on top of DCPG. Our algorithms achieve state-of-the-art observational generalization performance and sample efficiency compared to the prior model-free method on the Procgen benchmark [10].

2 Preliminaries

2.1 Observational Generalization in RL

We consider a collection of environments \mathcal{M} formulated as Markov Decision Processes (MDPs). Each environment $m \in \mathcal{M}$ is described as a tuple $(\mathcal{S}_m, \mathcal{A}, T_m, r_m, \rho_m, \gamma)$, where \mathcal{S}_m is the image-based state space, \mathcal{A} is the action space shared across all environments, $T_m : \mathcal{S}_m \times \mathcal{A} \rightarrow \mathcal{P}(\mathcal{S}_m)$ is the transition function, $r_m : \mathcal{S}_m \times \mathcal{A} \rightarrow \mathbb{R}$ is the reward function, ρ_m is the initial state distribution, and $\gamma \in [0, 1]$ is the discount factor. We assume that there exists visual variation in the state space between environments. While the transition and reward functions are defined as dependent on an environment, we assume that these functions share some common structures across all environments. A policy $\pi : \mathcal{S} \rightarrow \mathcal{P}(\mathcal{A})$ is trained using a fixed number of training environments $\mathcal{M}_{\text{train}} = \{m_i\}_{i=1}^n$, where \mathcal{S} is the set of all possible states in \mathcal{M} . The goal is to learn a generalizable policy that maximizes the expected return on the unseen test environments $\mathcal{M}_{\text{test}} = \mathcal{M} \setminus \mathcal{M}_{\text{train}}$.

In this paper, we use the Procgen benchmark as a testbed for evaluating observational generalization in RL [10]. The Procgen benchmark is a collection of 16 video games with high diversity comparable to the ALE benchmark [5]. Each game consists of procedurally generated environment instances with visually different layouts, backgrounds, and game entities (*e.g.*, the spawn locations and times for enemies), also called levels. The standard evaluation protocol on the Procgen benchmark is to train an agent using a finite set of training levels and evaluate the performance on held-out test levels [10].

2.2 Proximal Policy Optimization

Proximal Policy Optimization (PPO) is one of the most powerful model-free policy gradient methods, which learns a policy π_θ and value function V_ϕ parameterized by deep neural networks [40]. For training, PPO first collects trajectories τ using the old policy network $\pi_{\theta_{\text{old}}}$ right before the update. Then, the policy network π_θ is trained with the trajectories for several epochs, often called sample reuse, to maximize the following clipped surrogate policy objective J_π designed to constrain the size of policy update:

$$J_\pi(\theta) = \mathbb{E}_{s_t, a_t \sim \tau} \left[\min \left(\frac{\pi_\theta(a_t | s_t)}{\pi_{\theta_{\text{old}}}(a_t | s_t)} \hat{A}_t, \text{clip} \left(\frac{\pi_\theta(a_t | s_t)}{\pi_{\theta_{\text{old}}}(a_t | s_t)}, 1 - \epsilon, 1 + \epsilon \right) \hat{A}_t \right) \right],$$

where \hat{A}_t is an estimate of the advantage function at timestep t . The value network V_ϕ is trained with the trajectories to minimize the following value objective J_V :

$$J_V(\phi) = \mathbb{E}_{s_t \sim \tau} \left[\frac{1}{2} \left(V_\phi(s_t) - \hat{R}_t \right)^2 \right],$$

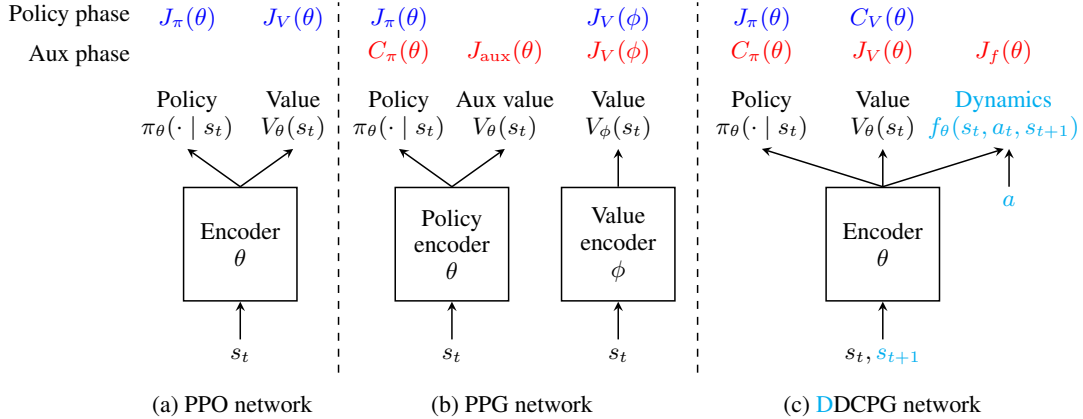


Figure 1: Network architectures for PPO, PPG, and DDCPG. The objectives J_π , J_V , J_{aux} , and J_f denote the policy, value, auxiliary value, and dynamics objectives, respectively. The regularizers C_π and C_V denote the policy and value regularizers, respectively. The blue and red terms define optimization problems during the policy and auxiliary phases, respectively.

where $\hat{R}_t = \hat{A}_t + V_\phi(s_t)$ is a value function target. It is used to compute the advantage estimates via generalized advantage estimator (GAE) [39].

In practice, the policy and value networks are jointly optimized with shared parameters (*i.e.*, $\theta = \phi$), especially in image-based RL [14, 44]. For example, they can be implemented using a shared encoder followed by separate linear heads, as shown in Figure 1a. Sharing parameters is advantageous in that representations learned by each objective can be beneficial to the other. It also reduces memory costs and accelerates training time. However, a shared network architecture complicates the optimization as a single encoder should be optimized over multiple objectives whose gradients may have varying scales and directions. It also constrains the policy and value networks to be optimized under the same training hyperparameter setting, such as batch size and the number of epochs, severely limiting the flexibility of PPO.

2.3 Phasic Policy Gradient

Phasic Policy Gradient (PPG) is an algorithm built upon PPO that significantly improves observational generalization by addressing the problems of sharing parameters [11]. More specifically, PPG employs separate encoders for the policy and value networks, as shown in Figure 1b. In addition, it introduces an auxiliary value head V_θ following the policy encoder to distill useful representations from the value network into the encoder. For training, PPG alternates between policy and auxiliary phases. During the policy phase, which is repeated N_π times, the policy and value networks are trained with newly-collected trajectories to optimize the policy and value objectives from PPO. Then, all states and value function targets in the trajectories are stored in a buffer \mathcal{B} . During the auxiliary phase, the auxiliary value head and the policy network are jointly trained with all data in the buffer to optimize the following auxiliary value objective J_{aux} and policy regularizer C_π :

$$J_{\text{aux}}(\theta) = \mathbb{E}_{s_t \sim \mathcal{B}} \left[\frac{1}{2} \left(V_\theta(s_t) - \hat{R}_t \right)^2 \right], \quad C_\pi(\theta) = \mathbb{E}_{s_t \sim \mathcal{B}} [D_{\text{KL}}(\pi_{\theta_{\text{old}}}(\cdot | s_t) \| \pi_\theta(\cdot | s_t))],$$

where $\pi_{\theta_{\text{old}}}$ is the policy network right before the auxiliary phase and D_{KL} denotes the KL divergence. In other words, the value network is distilled into the policy encoder while the outputs of the policy network are constrained to be unchanged. Moreover, the value network is additionally trained with all data in the buffer to optimize the value objective from PPO to obtain a more accurate value function. Note that the training data size in the auxiliary phase is N_π times larger than the policy phase. It has been claimed that the distillation of a better-trained value network with a separate architecture and the additional training for a more accurate value network can improve observational generalization performance and sample efficiency [11].

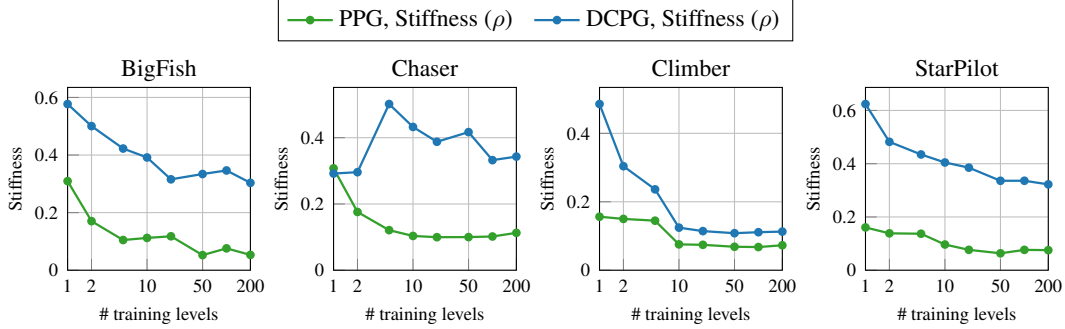


Figure 2: Stiffness of value objective gradients for PPG and DCPG on 4 Procgen games while varying the number of training levels.

3 Motivation

3.1 Overfitting in Value Network on Multiple Training Environments

We begin by investigating the difficulty of obtaining an accurate value network on multiple training environments. Indeed, learning a value network that better approximates the true value function on given training environments can lead to better training performance [42]. However, even in a simple setting where an agent is trained on a single environment, it has been shown that the value network is prone to overfitting in the sense that it does not extrapolate well even to unseen states of the same training environment [26, 23, 12, 17]. Increasing the number of training environments could further exacerbate this overfitting problem. Intuitively, the value network might rely more on memorization when fed fewer training samples per environment, given the same number of environment steps.

To corroborate this claim, we measure the stiffness of the value objective gradients between states (s, s') defined by

$$\rho(s, s') = \frac{\nabla_{\phi} J_V(\phi; s)^\top \nabla_{\phi} J_V(\phi; s')}{\|\nabla_{\phi} J_V(\phi; s)\|_2 \|\nabla_{\phi} J_V(\phi; s')\|_2},$$

following the practice in Fort et al. [18], Bengio et al. [6]. Low stiffness indicates that updating the network parameters toward minimizing the value objective for one state hurts minimizing the value objective for other states. It has also been shown that a value network with lower stiffness is more likely to memorize the training data [6]. More specifically, we train PPG agents on the Procgen games while varying the number of training levels from 0 to 200 and compute the average stiffness across all state pairs in a mini-batch of size 2^{14} ($=16,384$) throughout training. The detailed experimental settings and results can be found in Appendix A.

The green lines in Figure 2 show that the stiffness of the value objective gradients decreases as the number of training environments increases, as expected. It implies that the value network trained on multiple environments is more likely to memorize the training data and cannot accurately predict the values of unvisited states from the training environments. This overfitting problem brings us to train a value network with sufficient regularization.

3.2 Training Value Network with Explicit Regularization

Now, we examine the effectiveness of value network regularization in the multi-environment setting. We introduce two common approaches from the single-environment setting to prevent overfitting in a value network. First, discount regularization (DR) is a method that trains a value network with a lower discount factor γ' [34]. Second, activation regularization (AR) is a technique that trains a value network with L_2 penalty on its outputs:

$$J_V^{\text{reg}}(\phi) = \mathbb{E}_{s_t \sim \tau} \left[\frac{1}{2} \left(V_{\phi}(s_t) - \hat{R}_t \right)^2 + \frac{\alpha}{2} V_{\phi}(s_t)^2 \right],$$

where $\alpha > 0$ is the regularization coefficient [3].

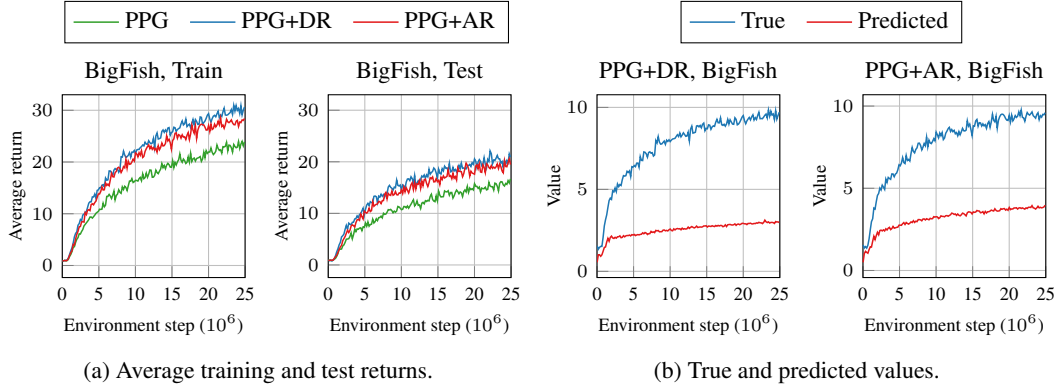


Figure 3: (a) Training and test performance curves of PPG, PPG+DR, and PPG+AR on BigFish. (b) True and predicted values measured at the initial states of training environments for PPG+DR and PPG+AR on BigFish. The mean is computed over 10 different runs.

To validate the effectiveness of the value network regularization in the multi-environment setting, we train PPG agents with each of these two methods using 200 training levels on the Procgen games. More specifically, we reduce the discount factor from $\gamma = 0.999$ to $\gamma' = 0.995$ for PPG+DR and use $\alpha = 0.05$ for PPG+AR. We measure the average training and test returns to evaluate the training performance and its transferability to unseen test environments.

As shown in Figure 3a, the value network regularization improves both the training and test performance of PPG to some extent. It implies that explicitly suppressing the value network also helps to reduce overfitting in the multi-environment setting. We also find that these regularization methods improve the training and test performance in all Procgen games on average. More details on the experimental setting and results can be found in Appendix B.

Despite its effectiveness, explicit value network regularization can lead to a suboptimal solution as the number of environment steps increases. Figure 3b shows the true and predicted values measured at the initial states of the training environments for PPG+DR and PPG+AR. We find that the value network trained with explicit regularization reaches a plateau too quickly, which implies that excessive regularization later hinders the value network from learning the exact value function. This motivates us to find a more flexible regularization that boosts training performance while allowing the value network to converge to true values.

4 Delayed-Critic Policy Gradient

In this section, we propose a new model-free policy gradient algorithm, namely *Delayed-Critic Policy Gradient* (DCPG), which deals with the overfitting problem of the value function in a simple and flexible way. The key idea is that the value network should be optimized less frequently than the policy network to suppress the value estimates and reduce overfitting. In addition, it should be trained with more data to prevent overfitting to small, recent training data, as mentioned in [29].

4.1 Algorithm

DCPG proceeds by alternating policy and auxiliary phases similar to PPG. Still, it employs a single unified network architecture in the same way as PPO and does not require any auxiliary value head, as shown in Figure 1c. During the policy phase, which occurs more frequently than the auxiliary phase but with less training data, the policy network is trained with newly-collected trajectories to optimize the policy objective from PPO. In contrast, the value network is constrained to preserve its outputs in the sense that updating the value network frequently with a small number of data can exacerbate the overfitting problem observed in Section 3.1 by optimizing the following value regularizer C_V :

$$C_V(\theta) = \mathbb{E}_{s_t \sim \tau} \left[\frac{1}{2} (V_\theta(s_t) - V_{\theta_{\text{old}}}(s_t))^2 \right],$$

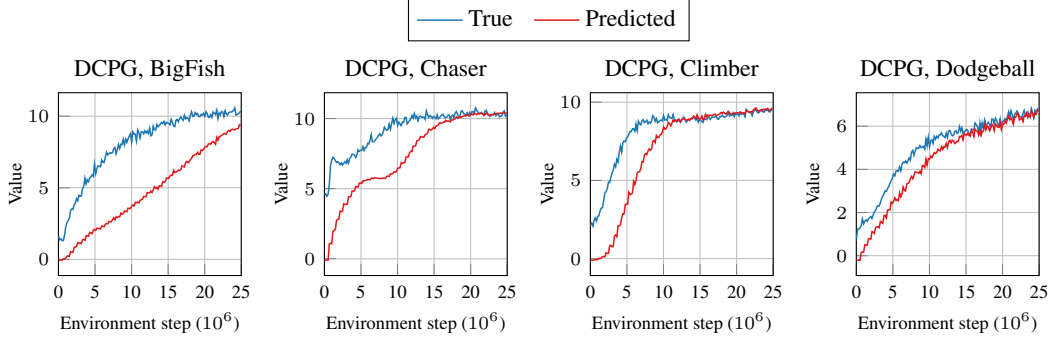


Figure 4: True and predicted values measured at the initial states of training environments for DCPG agents on 4 Procgen games. The mean is computed over 10 different runs.

where $V_{\theta_{\text{old}}}$ is the old value network right before the policy phase. Then, all states and value function targets in the trajectories are stored in a buffer.

During the auxiliary phase, the value network is trained with a larger number of data in the buffer to optimize the value objective from PPO. In contrast, the policy network is constrained to preserve its outputs by optimizing the policy regularizer. Note that since the value network shares the same encoder as the policy network, optimizing the value objective directly plays the role of representation learning for the policy network. Thus, unlike PPG, DCPG does not require an additional auxiliary head for feature distillation. The overall procedure of DCPG can be found in Algorithm 1.

Algorithm 1 Dynamics-aware Delayed-Critic Policy Gradient (DDCPG)

Require: Policy network π_θ , value network V_θ , dynamics discriminator f_θ

- 1: **for** phase = 1, 2, ... **do**
- 2: Initialize buffer \mathcal{B}
- 3: **for** iter = 1, 2, ..., N_π **do** ▷ Policy phase
- 4: Sample trajectories τ using π_θ and compute value function target \hat{R}_t for each state $s_t \in \tau$
- 5: **for** epoch = 1, 2, ..., E_π **do**
- 6: Optimize policy objective $J_\pi(\theta)$ and value regularizer $C_V(\theta)$ with τ
- 7: **end for**
- 8: Add (s_t, a_t, \hat{R}_t) to \mathcal{B}
- 9: **end for**
- 10: **for** iter = 1, 2, ..., E_{aux} **do** ▷ Auxiliary phase
- 11: Optimize value objective $J_V(\theta)$, dynamics objective $J_f(\theta)$, and policy regularizer $C_\pi(\theta)$ with \mathcal{B}
- 12: **end for**
- 13: **end for**

4.2 Value Network Analysis of Delayed Critic Update

The delayed critic update in DCPG can operate as implicit regularization of the value network. Since the policy improvement is not immediately reflected in the value network, it encourages smaller value estimates than the true values. To validate this claim, we train DCPG agents using 200 training levels on the Procgen games and measure the true and predicted values at the initial states of the training levels. Figure 4 shows the value estimates are kept lower than the true values at the early stage of training but recover the true values as training progresses. More results can be found in Appendix C.

We also evaluate the effectiveness of the delayed critic update in mitigating the overfitting problem by measuring the stiffness of the value function. The blue lines in Figure 2 show that DCPG has higher stiffness than PPG, implying that our value network is more robust against overfitting addressed in Section 3.1. We conclude that the delayed critic update in DCPG serves as a good regularizer for the value network. More results can be found in Appendix A.

4.3 Learning Forward and Inverse Dynamics with Single Discriminator

In the context of multi-task learning, learning an auxiliary task can serve as a regularizer that prevents overfitting in the main task [37]. Motivated by this, we consider learning an auxiliary task using the representations from the encoder and jointly learning the value network with the auxiliary objective. Suppose the buffer \mathcal{B} used in the auxiliary phase contains a transition tuple (s_t, a_t, s_{t+1}) . Since the transition function from each environment is assumed to have the same underlying structure, it is natural to train a neural network that models the forward dynamics of environments in the latent space of the encoder. Concretely, a dynamics head f_θ takes the embedding of the current state s_t and the current action a_t as inputs and predicts the embedding of the next state s_{t+1} . However, it is well known that a forward dynamics model using a neural network tends to overfit a small number of training data and make poor predictions on unseen states [8]. To address this, we consider learning the forward dynamics by training a discriminator that determines whether the next state is valid, given the current state and action:

$$f_\theta(s_t, a_t, s_{t+1}) = 1, f_\theta(s_t, a_t, \hat{s}_{t+1}) = 0, \hat{s}_{t+1} \in \mathcal{B} \setminus \{s_{t+1}\}.$$

Such a discriminator might discard information about the action to distinguish whether a transition is valid. For example, the discriminator can predict the valid transition by using only the proximity of the current and next states (see Appendix F for more details). To avoid this, we train the discriminator to jointly distinguish whether the current action is valid, given the current and next states (*i.e.*, inverse dynamics):

$$f_\theta(s_t, a_t, s_{t+1}) = 1, f_\theta(s_t, \hat{a}_t, s_{t+1}) = 0, \hat{a}_t \in \mathcal{A} \setminus \{a_t\}.$$

Finally, we optimize the following objective during the auxiliary phase:

$$J_f(\theta) = \mathbb{E}_{s_t, a_t, s_{t+1} \sim \mathcal{B}} \left[\log(f_\theta(s_t, a_t, s_{t+1})) + \log(1 - f_\theta(s_t, a_t, \hat{s}_{t+1})) \right. \\ \left. + \eta \log(1 - f_\theta(s_t, \hat{a}_t, s_{t+1})) \right],$$

where $\hat{s}_{t+1} \sim \mathcal{U}(\mathcal{B} \setminus \{s_{t+1}\})$, $\hat{a}_t \sim \mathcal{U}(\mathcal{A} \setminus \{a_t\})$, and $\eta > 0$ is the coefficient for the inverse dynamics. We name the resulting algorithm *Dynamics-aware Delayed-Critic Policy Gradient* (DDCPG). The network architecture and algorithm for DDCPG are shown in Figure 1c and Algorithm 1, respectively (the differences with DCPG are marked in cyan).

5 Experiments

5.1 Experimental Settings

We evaluate the observational generalization performance of our methods on the Procgen benchmark. We use the “easy” difficulty mode, which most prior works have focused on. We train agents on 200 training levels generated by seeds from 0 to 200 for 25M environment steps and test them on held-out test levels, following the practice in Cobbe et al. [10]. We measure the average return of 100 test episodes and report its mean and standard deviation over 10 runs with different initialization.

We compare our methods with PPO and 4 other baselines that use PPO as the backbone algorithm: UCB-DrAC, PLR, PPG, and DAAC [36, 24, 11, 35]. UCB-DrAC is a data augmentation algorithm for training policy and value networks to be robust against various transformations. PLR is a sampling algorithm for the procedural generation that selects the next training level based on its future learning potential. PPG is the previous state-of-the-art method on the Procgen benchmark. DAAC is motivated by PPG and distills the advantage function into the policy network instead. For each method, we use the same set of hyperparameters across all games, following the standard protocol in the ALE and Procgen benchmarks [32, 10]. For our methods, we use the same hyperparameter setting as PPG for a fair comparison. To compare the performance of each method with a single score, we calculate the PPO-normalized score averaged over all Procgen games, which is computed by dividing the average return of each method by PPO, following the practice in Jiang et al. [24], Raileanu et al. [36]. For the implementation details and hyperparameters, please refer to Appendix D. The code can be found at <https://github.com/snu-ml1ab/DCPG>.

5.2 Observational Generalization Performance on Procgen Benchmark

Table 1 shows the average test returns of each method on all 16 Procgen games. DCPG significantly outperforms all the baselines, yielding a 24%p improvement on average compared to the previous

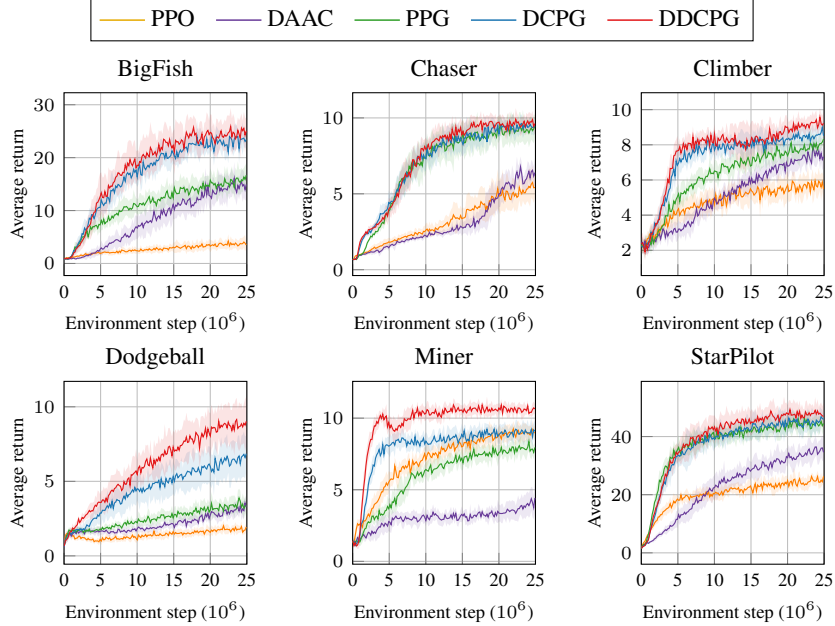


Figure 5: Test performance curves of each method on 6 Procgen games. Each agent is trained on 200 training levels for 25M environment steps and evaluated on 100 unseen test levels. The mean and standard deviation are computed over 10 different runs.

Table 1: Average test returns of each method on all 16 Procgen games. Each agent is trained on 200 training levels for 25M environment steps and evaluated on 100 unseen test levels. The mean and standard deviation are computed over 10 different runs.

Environment	PPO	UCB-DrAC	PLR	DAAC ²	PPG	DCPG	DDCPG
BigFish	3.4 ± 1.0	6.6 ± 2.5	10.8 ± 2.5	15.3 ± 3.0	16.4 ± 2.0	23.1 ± 2.3	25.9 ± 2.3
BossFight	7.4 ± 0.7	7.2 ± 1.0	8.8 ± 0.7	9.5 ± 0.8	10.4 ± 0.6	10.2 ± 0.4	10.6 ± 0.5
CaveFlyer	5.2 ± 0.6	4.4 ± 0.8	6.3 ± 0.7	5.1 ± 0.6	7.7 ± 0.7	6.3 ± 0.4	6.0 ± 0.3
Chaser	5.5 ± 0.8	6.7 ± 0.5	7.5 ± 0.8	6.3 ± 0.8	8.9 ± 0.9	9.7 ± 0.4	9.9 ± 0.6
Climber	5.5 ± 0.6	6.2 ± 0.6	6.4 ± 0.5	7.4 ± 0.5	8.1 ± 0.4	8.5 ± 0.7	9.3 ± 0.7
CoinRun	8.8 ± 0.3	8.6 ± 0.4	8.9 ± 0.3	9.3 ± 0.2	8.9 ± 0.3	8.5 ± 0.4	8.4 ± 0.3
Dodgeball	1.9 ± 0.3	4.5 ± 1.4	2.2 ± 0.4	3.2 ± 0.5	3.6 ± 0.7	6.7 ± 0.4	9.0 ± 1.6
FruitBot	27.5 ± 1.5	26.9 ± 1.7	27.7 ± 1.3	28.5 ± 1.4	29.1 ± 1.0	29.0 ± 1.2	28.8 ± 0.6
Heist	2.6 ± 0.6	3.4 ± 1.0	3.1 ± 0.6	3.0 ± 0.5	2.8 ± 0.5	3.3 ± 0.5	4.4 ± 0.8
Jumper	5.7 ± 0.4	5.6 ± 0.4	5.9 ± 0.4	5.8 ± 0.4	6.0 ± 0.4	6.2 ± 0.5	6.4 ± 0.4
Leaper	5.6 ± 1.5	3.6 ± 0.7	7.3 ± 0.2	8.2 ± 1.1	7.2 ± 2.4	6.9 ± 1.7	6.8 ± 1.5
Maze	5.3 ± 0.7	5.7 ± 1.1	5.6 ± 0.5	5.6 ± 0.6	5.3 ± 0.4	5.7 ± 0.7	6.5 ± 0.6
Miner	9.2 ± 0.6	10.1 ± 0.7	9.4 ± 0.7	4.4 ± 1.1	7.6 ± 0.7	9.1 ± 0.8	10.6 ± 0.5
Ninja	5.7 ± 0.5	5.7 ± 0.5	7.1 ± 0.5	6.7 ± 0.7	6.7 ± 0.4	6.3 ± 0.6	6.6 ± 0.5
Plunder	5.0 ± 0.5	8.1 ± 1.5	8.7 ± 1.3	5.6 ± 0.6	13.7 ± 1.7	13.7 ± 1.3	12.9 ± 2.5
StarPilot	25.8 ± 2.0	27.0 ± 3.2	24.9 ± 3.6	35.9 ± 3.3	44.8 ± 2.6	46.1 ± 2.1	46.6 ± 4.1
PPO-norm score (%)	100.0 ± 3.1	120.7 ± 10.7	130.0 ± 6.0	136.7 ± 7.6	160.3 ± 6.3	184.5 ± 5.2	202.2 ± 10.2

state-of-the-art PPG. Adding dynamics learning to DCPG can further improve the test performance with an 18%p increase in the PPO-normalized score. We also provide the average training returns on all Procgen games in Appendix E, showing that our methods achieve better sample efficiency in the multi-environment setting. Furthermore, we evaluate the performance of our methods using the Min-Max normalized score and report mean, median, and interquartile mean (IQM) scores in Appendix G, following the recent practice in Agarwal et al. [2]. We observe that the performance improvements of our methods are statistically significant for all the metrics we consider.

Figure 5 shows the test performance curves of each method on 6 Procgen games throughout training. Our methods achieve superior final test performance and acquire generalization ability with fewer environment interactions. For example, our methods can reach the final performance of PPG using

²Results reported in the original paper use a different hyperparameter setting for each game.

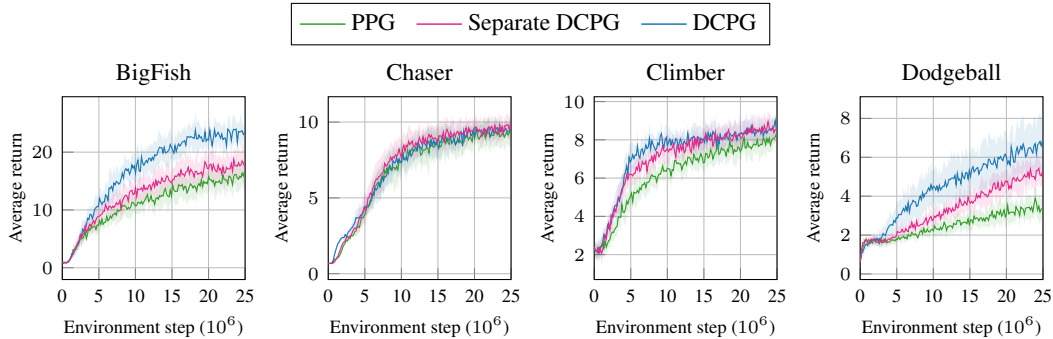


Figure 6: Test performance curves of PPG, Separate DCPG, and DCPG on 4 Progen games. Each agent is trained on 200 training levels for 25M environment steps and evaluated on 100 unseen test levels. The mean and standard deviation are computed over 10 different runs.

only 20% of total environment steps in BigFish and Climber and 10% in Dodgeball and Miner. More experimental results can be found in Appendix E.

5.3 Ablation Study for Delayed Critic Update

The delayed critic update not only alleviates the overfitting problem but also provides better representations for generalization to the policy network. To validate this, we train DCPG agents with an additional value network V_ϕ using a separate encoder (Separate DCPG). The separate value network V_ϕ is aggressively optimized in the same way as PPG and only used for calculating advantages in the policy objective. The original value network V_θ is only used for learning representations for the policy network with delayed updates. Figure 6 shows that Separate DCPG achieves better test performance than PPG, implying that the delayed critic update produces more generalizable representations. For the detailed experimental settings and results, please refer to Appendix F.

5.4 Ablation Study for Dynamics Learning

We conduct an ablation study to show the effectiveness of training forward and inverse dynamics using a single discriminator. We train DCPG agents with only forward dynamics learning (DCPG+F) and only inverse dynamics learning (DCPG-I). In addition, we train DCPG agents with forward and inverse dynamics learning using two separate discriminators (DCPG+FI). Table 2 shows that DDCPG, which jointly optimizes the forward and inverse dynamics with a single discriminator, achieves better test performance than the other methods with dynamics learning. Note that inverse dynamics provides performance gain only when jointly trained with forward dynamics using a single discriminator. We provide the detailed experimental settings and results in Appendix F.

Table 2: PPO-normalized score of each method with dynamics learning on all 16 Progen games. Each agent is trained on 200 training levels for 25M environment steps and evaluated on 100 unseen test levels. The mean and standard deviation are computed over 10 different runs.

	DCPG	DCPG+F	DCPG-I	DCPG+FI	DDCPG
PPO-norm score (%)	184.5 ± 5.2	195.9 ± 7.7	185.5 ± 6.5	194.6 ± 6.2	202.2 ± 10.2

6 Related Works

Observational generalization in RL One prominent approach for improving observational generalization in model-free RL is to employ regularization techniques developed for supervised learning, such as batch normalization, weight regularization, and information bottleneck [16, 9, 22]. Several works adopt data augmentation strategies commonly used in computer vision to address the generalization problem [28, 43]. For example, UCB-DrAC proposes a method that automatically finds an effective augmentation and introduces new regularization terms to learn robust state representations

under various image transformations [36]. Recently, it has been shown that MuZero Reanalyse, the state-of-the-art model-based RL algorithm, achieves better observational generalization performance than model-free approaches, though it requires a larger network architecture [4].

Another line of work uses self-supervised learning to learn invariant representations that can generalize to unseen environments. Some methods attempt to learn state representations that capture long-term behavior proximity between states using bisimulation or policy similarity metrics to discard irrelevant information for generalization [45, 1, 31]. The idea of learning dynamics as a self-supervised task, originally developed for sample efficiency, has also been used to improve observational generalization [20, 41]. DIM learns a state representation that can predict the representations of successive timesteps using self-supervised learning [30]. It has also been tested that predicting future state representations conditioned on the current state and action improves the generalization performance of MuZero [4]. Our work aims to enhance dynamics learning further by jointly modeling the forward and inverse dynamics objectives using a single discriminator.

PPG is most closely related to our work, which proposes a better training algorithm to improve both observational generalization and sample efficiency in the multi-environment setting [11]. It trains the policy and value networks using a separate architecture with different levels of sample reuse to avoid interference and obtain a better-trained value network. DAAC also uses decoupled policy and value networks for a more accurate value function but distills the advantage function into the policy encoder under the assumption that it is less prone to overfitting to environment-specific features than the value function [35]. In contrast, we focus on regularizing the value network while obtaining better representation, which distinguishes our work from the prior methods.

Learning value networks with regularization Discount regularization is one common regularization method to mitigate overfitting in the value network [7]. A lower discount factor can lead to better performance in approximated dynamic programming when the approximation error is large [34]. It is also helpful for preventing overfitting when dealing with limited data in POMDPs [19]. Activation regularization penalizes the outputs of the value network and has a regularization effect similar to that of discount regularization [3]. It has been shown that activation regularization is equivalent to discount regularization in batch TD learning and also effective in online RL [3].

7 Conclusion

We have investigated the difficulty of learning an accurate value network in the multi-environment setting and shown that suppressing the value network with appropriate regularization can be helpful to improve both the training and test performance. Based on this observation, we propose Delayed-Critic Policy Gradient (DCPG), where the value network is implicitly regularized to have lower predicted values at the early stage of training with delayed updates compared to the policy network. We find that the delayed value update prevents the memorization of training data and produces more generalizable representations that can be extended to unseen test environments. Furthermore, we introduce a simple self-supervised task that jointly learns forward and inverse dynamics using a single discriminator, which can be easily combined with DCPG. Our methods exhibit state-of-the-art performance in observational generalization on the challenging Procgen benchmark.

Acknowledgements

This work was supported in part by Samsung Advanced Institute of Technology, Samsung Electronics Co., Ltd., Institute of Information & Communications Technology Planning & Evaluation (IITP) grant funded by the Korea government (MSIT) (No. 2019-0-01371, Development of brain-inspired AI with human-like intelligence, No. 2020-0-00882, (SW STAR LAB) Development of deployable learning intelligence via self-sustainable and trustworthy machine learning, and No. 2022-0-00480, Development of Training and Inference Methods for Goal-Oriented Artificial Intelligence Agents), and a grant of the Korea Health Technology R&D Project through the Korea Health Industry Development Institute (KHIDI), funded by the Ministry of Health & Welfare, Republic of Korea (grant number: HI21C1074). This material is based upon work supported by the Air Force Office of Scientific Research under award number FA2386-22-1-4010. Hyun Oh Song is the corresponding author.

References

- [1] Rishabh Agarwal, Marlos C. Machado, Pablo Samuel Castro, and Marc G Bellemare. Contrastive behavioral similarity embeddings for generalization in reinforcement learning. In *ICLR*, 2021.
- [2] Rishabh Agarwal, Max Schwarzer, Pablo Samuel Castro, Aaron C Courville, and Marc Bellemare. Deep reinforcement learning at the edge of the statistical precipice. In *NeurIPS*, 2021.
- [3] Ron Amit, Ron Meir, and Kamil Ciosek. Discount factor as a regularizer in reinforcement learning. In *ICML*, 2020.
- [4] Ankesh Anand, Jacob C Walker, Yazhe Li, Eszter Vertes, Julian Schrittwieser, Sherjil Ozair, Theophane Weber, and Jessica B Hamrick. Procedural generalization by planning with self-supervised world models. In *ICLR*, 2022.
- [5] Marc G Bellemare, Yavar Naddaf, Joel Veness, and Michael Bowling. The arcade learning environment: An evaluation platform for general agents. *Journal of Artificial Intelligence Research*, 47:253–279, 2013.
- [6] Emmanuel Bengio, Joelle Pineau, and Doina Precup. Interference and generalization in temporal difference learning. In *ICML*, 2020.
- [7] D. P. Bertsekas and J. N. Tsitsiklis. *Neuro-dynamic programming*. Athena Scientific, Belmont, MA, 1996.
- [8] Kurtland Chua, Roberto Calandra, Rowan McAllister, and Sergey Levine. Deep reinforcement learning in a handful of trials using probabilistic dynamics models. In *NeurIPS*, 2018.
- [9] Karl Cobbe, Oleg Klimov, Chris Hesse, Taehoon Kim, and John Schulman. Quantifying generalization in reinforcement learning. In *ICML*, 2019.
- [10] Karl Cobbe, Chris Hesse, Jacob Hilton, and John Schulman. Leveraging procedural generation to benchmark reinforcement learning. In *ICML*, 2020.
- [11] Karl W Cobbe, Jacob Hilton, Oleg Klimov, and John Schulman. Phasic policy gradient. In *ICML*, 2021.
- [12] Will Dabney, Andre Barreto, Mark Rowland, Robert Dadashi, John Quan, Marc G Bellemare, and David Silver. The value-improvement path: Towards better representations for reinforcement learning. In *AAAI*, 2021.
- [13] Felix Dangel, Frederik Kunstner, and Philipp Hennig. BackPACK: Packing more into backprop. In *ICLR*, 2020.
- [14] Prafulla Dhariwal, Christopher Hesse, Oleg Klimov, Alex Nichol, Matthias Plappert, Alec Radford, John Schulman, Szymon Sidor, Yuhuai Wu, and Peter Zhokhov. Openai baselines. <https://github.com/openai/baselines>, 2017.
- [15] Lasse Espeholt, Hubert Soyer, Remi Munos, Karen Simonyan, Vlad Mnih, Tom Ward, Yotam Doron, Vlad Firoiu, Tim Harley, Iain Dunning, et al. Impala: Scalable distributed deep-rl with importance weighted actor-learner architectures. In *ICML*, 2018.
- [16] Jesse Farebrother, Marlos C Machado, and Michael Bowling. Generalization and regularization in dqn. *arXiv preprint arXiv:1810.00123*, 2018.
- [17] Yannis Flet-Berliac, reda ouhanna, odalric-ambrym maillard, and Philippe Preux. Learning value functions in deep policy gradients using residual variance. In *ICLR*, 2021.
- [18] Stanislav Fort, Paweł Krzysztof Nowak, Stanislaw Jastrzebski, and Sridhar Narayanan. Stiffness: A new perspective on generalization in neural networks. *arXiv preprint arXiv:1901.09491*, 2019.
- [19] Vincent Franois-Lavet, Guillaume Rabusseau, Joelle Pineau, Damien Ernst, and Raphael Fonteneau. On overfitting and asymptotic bias in batch reinforcement learning with partial observability. *Journal of Artificial Intelligence Research*, 65:1–30, 2019.

- [20] Carles Gelada, Saurabh Kumar, Jacob Buckman, Ofir Nachum, and Marc G Bellemare. Deepmdp: Learning continuous latent space models for representation learning. In *ICML*, 2019.
- [21] Tuomas Haarnoja, Aurick Zhou, Pieter Abbeel, and Sergey Levine. Soft actor-critic: Off-policy maximum entropy deep reinforcement learning with a stochastic actor. In *ICML*, 2018.
- [22] Maximilian Igl, Kamil Ciosek, Yingzhen Li, Sebastian Tschitschek, Cheng Zhang, Sam Devlin, and Katja Hofmann. Generalization in reinforcement learning with selective noise injection and information bottleneck. In *NeurIPS*, 2019.
- [23] Andrew Ilyas, Logan Engstrom, Shibani Santurkar, Dimitris Tsipras, Firdaus Janoos, Larry Rudolph, and Aleksander Madry. A closer look at deep policy gradients. In *ICLR*, 2020.
- [24] Minqi Jiang, Edward Grefenstette, and Tim Rocktäschel. Prioritized level replay. In *ICML*, 2021.
- [25] Diederik P Kingma and Jimmy Ba. Adam: A method for stochastic optimization. *arXiv preprint arXiv:1412.6980*, 2014.
- [26] J Zico Kolter and Andrew Y Ng. Regularization and feature selection in least-squares temporal difference learning. In *ICML*, 2009.
- [27] Ilya Kostrikov. Pytorch implementations of reinforcement learning algorithms. <https://github.com/ikostrikov/pytorch-a2c-ppo-acktr-gail>, 2018.
- [28] Misha Laskin, Kimin Lee, Adam Stooke, Lerrel Pinto, Pieter Abbeel, and Aravind Srinivas. Reinforcement learning with augmented data. In *NeurIPS*, 2020.
- [29] Nir Levine, Tom Zahavy, Daniel J Mankowitz, Aviv Tamar, and Shie Mannor. Shallow updates for deep reinforcement learning. In *NeurIPS*, 2017.
- [30] Bogdan Mazouze, Remi Tachet des Combes, Thang Long Doan, Philip Bachman, and R Devon Hjelm. Deep reinforcement and infomax learning. In *NeurIPS*, 2020.
- [31] Bogdan Mazouze, Ahmed M Ahmed, R Devon Hjelm, Andrey Kolobov, and Patrick MacAlpine. Cross-trajectory representation learning for zero-shot generalization in RL. In *ICLR*, 2022.
- [32] Volodymyr Mnih, Koray Kavukcuoglu, David Silver, Andrei A Rusu, Joel Veness, Marc G Bellemare, Alex Graves, Martin Riedmiller, Andreas K Fidjeland, Georg Ostrovski, et al. Human-level control through deep reinforcement learning. *nature*, 518(7540):529–533, 2015.
- [33] Adam Paszke, Sam Gross, Francisco Massa, Adam Lerer, James Bradbury, Gregory Chanan, Trevor Killeen, Zeming Lin, Natalia Gimelshein, Luca Antiga, et al. Pytorch: An imperative style, high-performance deep learning library. In *NeurIPS*, 2019.
- [34] Marek Petrik and Bruno Scherrer. Biasing approximate dynamic programming with a lower discount factor. In *NeurIPS*, 2008.
- [35] Roberta Raileanu and Rob Fergus. Decoupling value and policy for generalization in reinforcement learning. In *ICML*, 2021.
- [36] Roberta Raileanu, Maxwell Goldstein, Denis Yarats, Ilya Kostrikov, and Rob Fergus. Automatic data augmentation for generalization in reinforcement learning. In *NeurIPS*, 2021.
- [37] Sebastian Ruder. An overview of multi-task learning in deep neural networks. *arXiv preprint arXiv:1706.05098*, 2017.
- [38] Julian Schrittwieser, Ioannis Antonoglou, Thomas Hubert, Karen Simonyan, Laurent Sifre, Simon Schmitt, Arthur Guez, Edward Lockhart, Demis Hassabis, Thore Graepel, et al. Mastering atari, go, chess and shogi by planning with a learned model. *Nature*, 588(7839):604–609, 2020.
- [39] John Schulman, Philipp Moritz, Sergey Levine, Michael Jordan, and Pieter Abbeel. High-dimensional continuous control using generalized advantage estimation. In *ICLR*, 2016.

- [40] John Schulman, Filip Wolski, Prafulla Dhariwal, Alec Radford, and Oleg Klimov. Proximal policy optimization algorithms. *arXiv preprint arXiv:1707.06347*, 2017.
- [41] Max Schwarzer, Ankesh Anand, Rishab Goel, R Devon Hjelm, Aaron Courville, and Philip Bachman. Data-efficient reinforcement learning with self-predictive representations. In *ICLR*, 2021.
- [42] Richard S Sutton, David McAllester, Satinder Singh, and Yishay Mansour. Policy gradient methods for reinforcement learning with function approximation. In *NeurIPS*, 1999.
- [43] Denis Yarats, Ilya Kostrikov, and Rob Fergus. Image augmentation is all you need: Regularizing deep reinforcement learning from pixels. In *ICLR*, 2021.
- [44] Denis Yarats, Amy Zhang, Ilya Kostrikov, Brandon Amos, Joelle Pineau, and Rob Fergus. Improving sample efficiency in model-free reinforcement learning from images. In *AAAI*, 2021.
- [45] Amy Zhang, Rowan Thomas McAllister, Roberto Calandra, Yarín Gal, and Sergey Levine. Learning invariant representations for reinforcement learning without reconstruction. In *ICLR*, 2021.
- [46] Chiyuan Zhang, Oriol Vinyals, Remi Munos, and Samy Bengio. A study on overfitting in deep reinforcement learning. *arXiv preprint arXiv:1804.06893*, 2018.

Checklist

1. For all authors...
 - (a) Do the main claims made in the abstract and introduction accurately reflect the paper’s contributions and scope? **[Yes]** We clearly reflect the main claims in Section 3 and Section 4.
 - (b) Did you describe the limitations of your work? **[N/A]**
 - (c) Did you discuss any potential negative societal impacts of your work? **[N/A]**
 - (d) Have you read the ethics review guidelines and ensured that your paper conforms to them? **[Yes]** We have read the ethics review guidelines and checked our paper has no conflict.
2. If you are including theoretical results...
 - (a) Did you state the full set of assumptions of all theoretical results? **[N/A]**
 - (b) Did you include complete proofs of all theoretical results? **[N/A]**
3. If you ran experiments...
 - (a) Did you include the code, data, and instructions needed to reproduce the main experimental results (either in the supplemental material or as a URL)? **[Yes]** We provide the code for reproducing the main results in the supplementary material.
 - (b) Did you specify all the training details (e.g., data splits, hyperparameters, how they were chosen)? **[Yes]** We provide the implementation details and hyperparameters of all baselines and our methods in the supplementary material.
 - (c) Did you report error bars (e.g., with respect to the random seed after running experiments multiple times)? **[Yes]** We conduct experiments over 10 training seeds and report mean and standard deviation.
 - (d) Did you include the total amount of compute and the type of resources used (e.g., type of GPUs, internal cluster, or cloud provider)? **[Yes]** We describe the computational resource in the supplementary material.
4. If you are using existing assets (e.g., code, data, models) or curating/releasing new assets...
 - (a) If your work uses existing assets, did you cite the creators? **[Yes]** We cite the benchmark used for our experiments.
 - (b) Did you mention the license of the assets? **[N/A]**
 - (c) Did you include any new assets either in the supplemental material or as a URL? **[N/A]**

- (d) Did you discuss whether and how consent was obtained from people whose data you're using/curating? [N/A]
 - (e) Did you discuss whether the data you are using/curating contains personally identifiable information or offensive content? [N/A]
5. If you used crowdsourcing or conducted research with human subjects...
- (a) Did you include the full text of instructions given to participants and screenshots, if applicable? [N/A]
 - (b) Did you describe any potential participant risks, with links to Institutional Review Board (IRB) approvals, if applicable? [N/A]
 - (c) Did you include the estimated hourly wage paid to participants and the total amount spent on participant compensation? [N/A]

A Stiffness Analysis

To quantify how much the number of training environments affects the overfitting in the value network, we train PPG agents using the training levels of seeds from 0 to n for 8M environment steps on all 16 Procgen games and measure the stiffness of the value objective gradients between states while varying the number of training environments $n \in \{1, 2, 5, 10, 20, 50, 100, 200\}$. Throughout the training, we sample trajectories from the training levels, which consist of 2^{14} (=16,384) states, and compute the individual value objective gradient for each state using BackPACK [13]. Then, we calculate the mean stiffness of the gradients across all state pairs and report its average computed over all training epochs.

The green lines in Figure 7 demonstrate that the stiffness decreases as the number of training levels increases in most of the Procgen games. This implies that a value network trained on more training environments is more likely to memorize training data and cannot extrapolate values of unseen states from the training environments.

We also conduct stiffness experiments for DCPG agents under the same experimental setting as PPG to evaluate how the delayed value update mitigates the overfitting problem. The blue lines in Figure 7 show that DCPG achieves higher stiffness than PPG for all n in 12 of 16 Procgen games. This suggests that the delayed value update effectively alleviates the memorization problem.

B Training Value Function with Explicit Regularization

We train PPG agents with discount regularization (PPG+DR) and activation regularization (PPG+AR) using 200 training levels for 25M environment steps on all 16 Procgen games and report the PPO-normalized training and test scores. For PPG+DR, we sweep the new discount factor γ' in a range of $\{0.98, 0.99, 0.995\}$ and find $\gamma' = 0.995$ performs best. For PPG+AR, we sweep the regularization coefficient α within $\{0.01, 0.05, 0.1\}$ and find $\alpha = 0.05$ works best. Table 3 shows that PPG+DR and PPG+AR improve both the training and test scores of PPG by 10%p.

Table 3: PPO-normalized training and test scores of PPG, PPG+DR, and PPG+AR. Each agent is trained on 200 training levels for 25M environment steps. The mean and standard deviation are computed over 10 different runs.

	PPG	PPG+DR	PPG+AR
PPO-norm train score (%)	136.7 ± 4.4	146.8 ± 1.4	146.7 ± 2.6
PPO-norm test score (%)	160.3 ± 6.3	168.0 ± 5.8	169.9 ± 6.9

C Value Network Analysis of Delayed Critic Update

To verify whether the delayed critic update acts as a value network regularizer, we train DCPG agents using 200 training levels for 25M environment steps on all 16 games of Procgen and compare the true and predicted values for the initial states of the training levels. More specifically, we collect 100 training episodes throughout the training and evaluate the value network prediction for the initial state of each trajectory. We estimate the true value of each initial state by computing the discounted return of the corresponding trajectory. We also conduct the same experiments with PPG+DR and PPG+AR for comparison with explicit value function regularization.

The red curves in Figure 8 show that the value network of DCPG consistently underestimates the true values when the number of environment steps is small. In addition, the value predictions of DCPG become less biased as training progresses and reach the true values in most games. It implies that the delayed value update can serve as implicit regularization that slowly diminishes in strength, which can be beneficial both in the early and late stages of training. In contrast, the value network trained with discount and activation regularization fails to make unbiased predictions even at the end of the training, as shown in Figures 9 and 10.

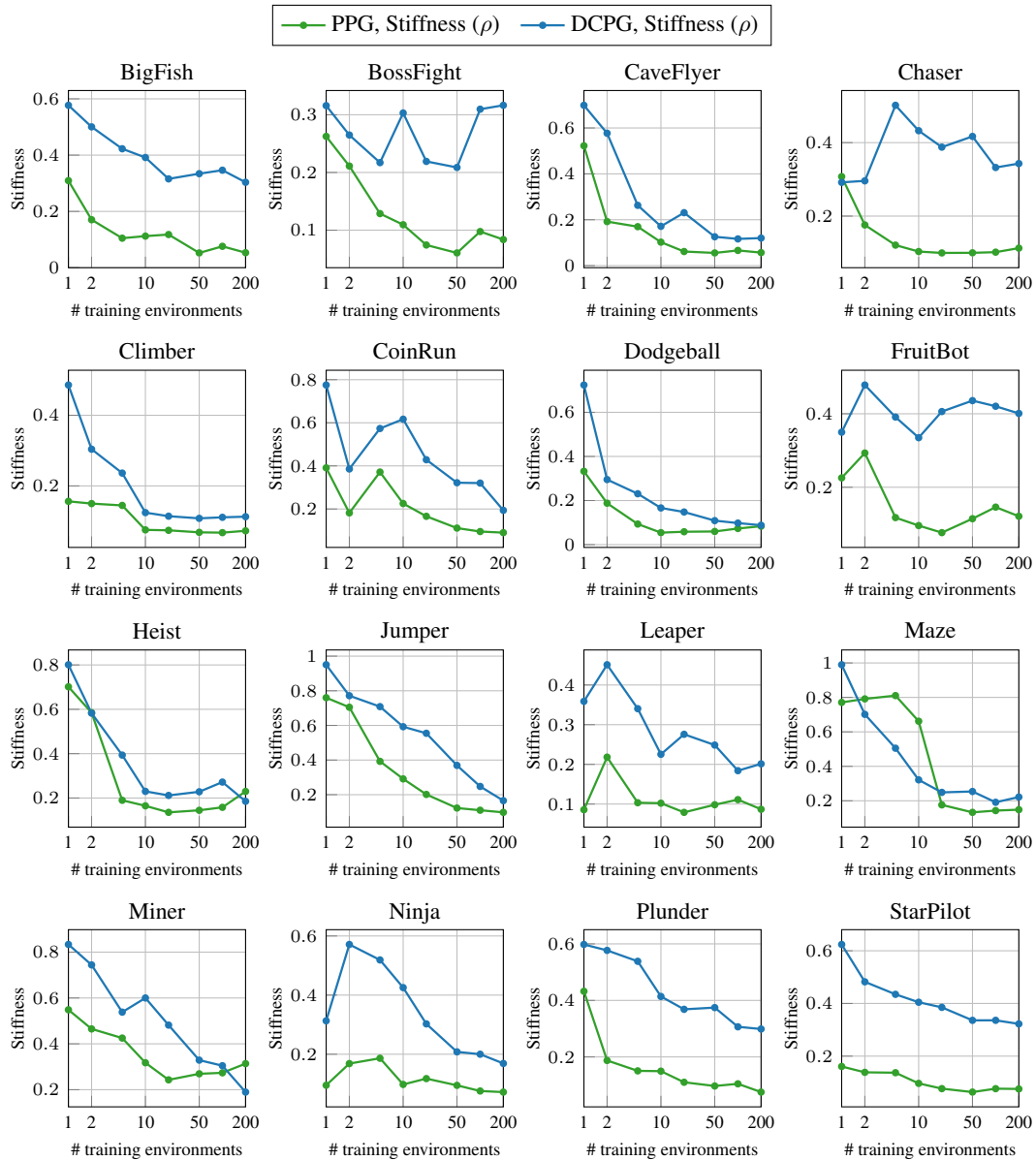


Figure 7: Stiffness of value objective gradients for PPG and DCPG while varying the number of training levels on all 16 Procgen games. Each agent is trained for 8M environment steps.

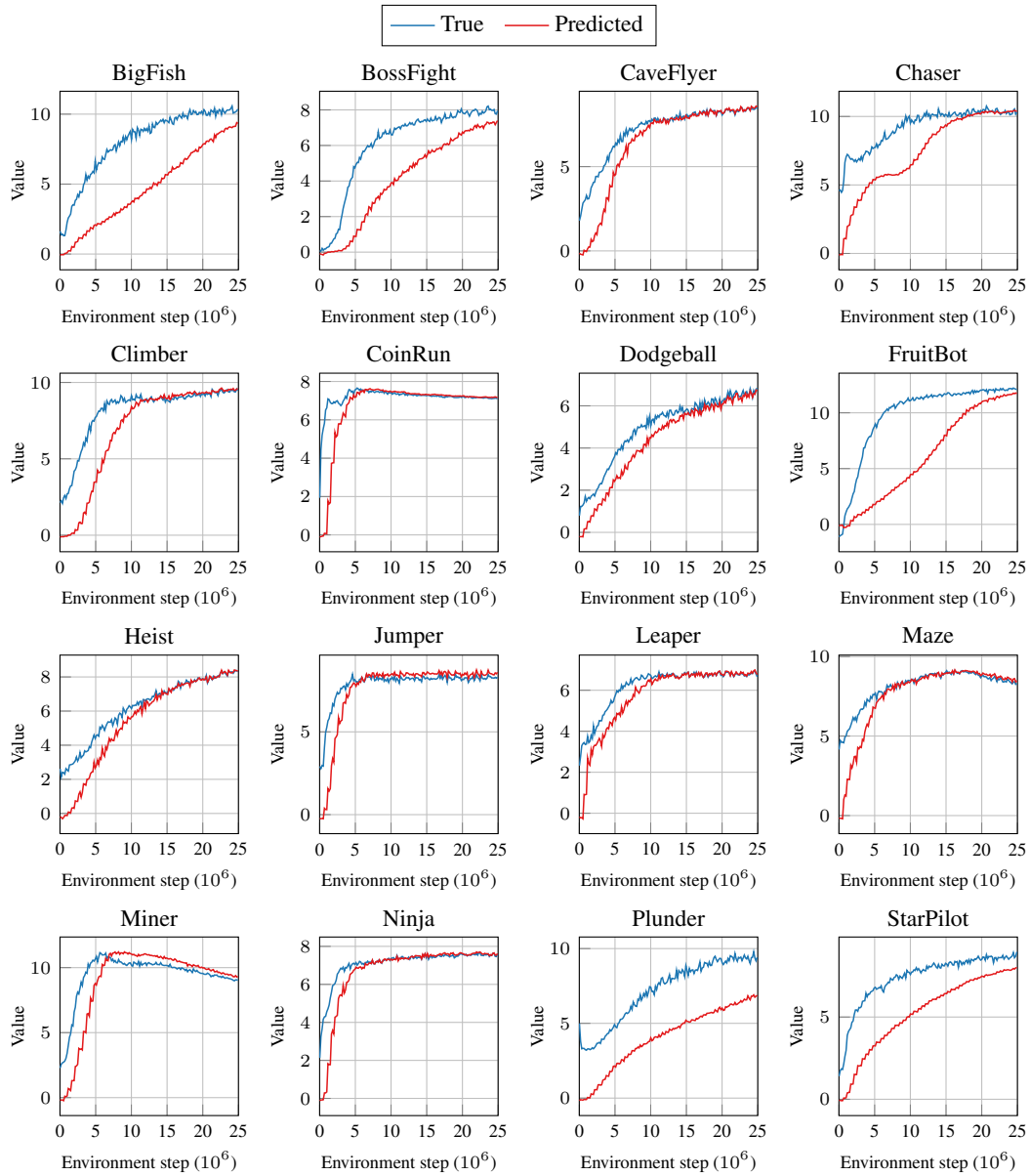


Figure 8: True and predicted values measured at the initial states of training environments for DCPG on all 16 Procgen games. The mean is computed over 10 different runs.

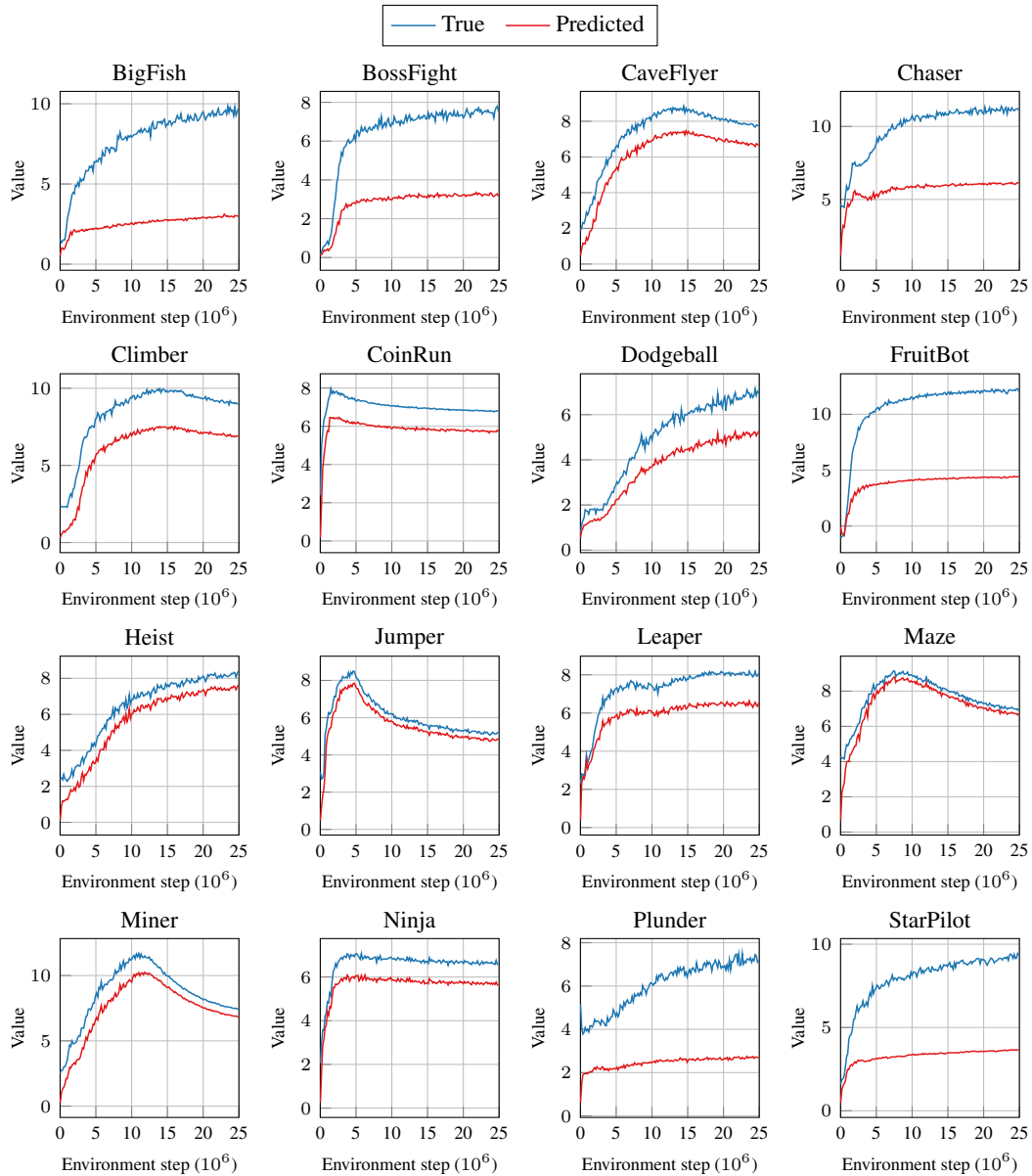


Figure 9: True and predicted values measured at the initial states of training environments for PPG with discount regularization (PPG+DR) on all 16 Procgen games. The mean is computed over 10 different runs.

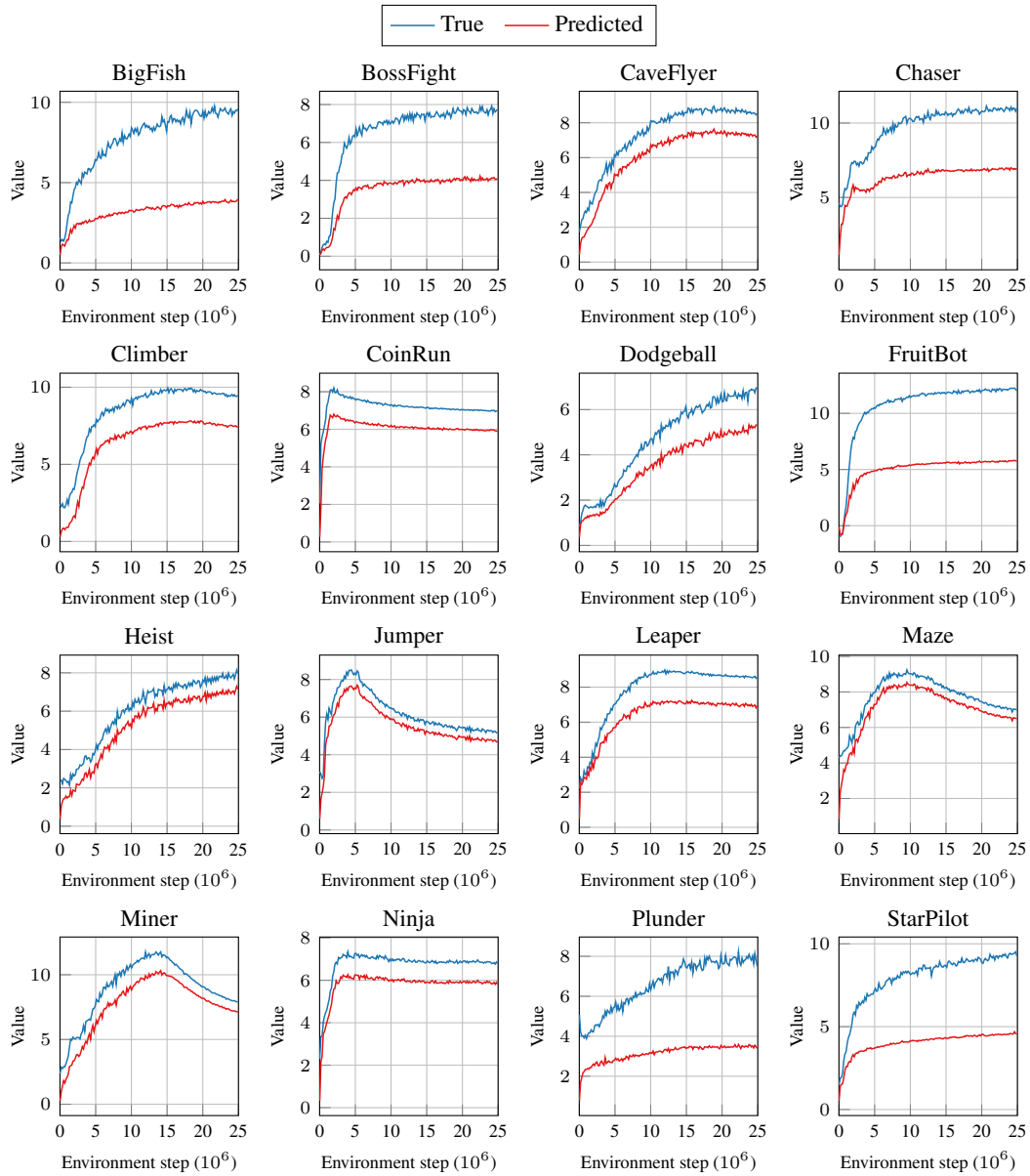


Figure 10: True and predicted values measured at the initial states of training environments for PPG with activation regularization (PPG+AR) on all 16 Procgen games. The mean is computed over 10 different runs.

D Implementation Details & Hyperparameters

For all experiments, we implement policy and value networks using the ResNet architecture proposed in IMPALA [15] and train the networks using Adam optimizer [25], following the standard practice in the prior works [10, 11]. We conduct all experiments using Intel Xeon Gold 5220R CPU, 64GB RAM, and NVIDIA RTX 2080 Ti GPU. We use PyTorch as a deep learning framework [33].

PPO We use the implementation of PPO by Kostrikov [27]. Unless otherwise specified, we use the same hyperparameter setting provided in Cobbe et al. [10] to reproduce PPO and PPO-based methods. The values of the hyperparameters used are shown in Table 4.

Table 4: PPO hyperparameters.

Hyperparameter	Value
Discount factor (γ)	0.999
GAE smoothing parameter (λ)	0.95
# timesteps per rollout	256
# epochs per rollout	3
# minibatches per epoch	8
Entropy bonus	0.01
PPO clip range (ϵ)	0.2
Reward normalization?	Yes
Learning rate	5e-4
# workers	1
# environments per worker	64
Total timesteps	25M
LSTM?	No
Frame stack?	No

UCB-DrAC We use the official implementation by the authors³. We use the best hyperparameter setting provided in the original paper. More specifically, we use regularization coefficient $\alpha_r = 0.1$, exploration coefficient $c = 0.1$, and sliding window size $K = 10$ for all Procgen games.

PLR We reproduce the reported results of PLR using the implementation released by the authors⁴. We use the recommended hyperparameter setting presented in the original paper and use L_1 value loss as the scoring function, rank prioritization, temperature $\beta = 0.1$, and staleness coefficient $\rho = 0.1$ for all Procgen games.

PPG We build PPG on top of the implementation of PPO. For PPO hyperparameters, we use the default hyperparameter setting in Table 4, except for the number of PPO epochs. For PPG-specific hyperparameters, we use the best hyperparameter setting provided in Cobbe et al. [11]. The values of the PPG-specific hyperparameter are shown in Table 5. The policy regularizer coefficient β_π denotes the weight for the policy regularizer C_π when jointly optimized with the auxiliary objective J_{aux} . We also provide the pseudocode of PPG in Algorithm 2.

DAAC For DAAC and IDAAC, which adds an auxiliary regularizer to the DAAC policy network, we use the official code released by the authors⁵. We find that some hyperparameters should be set differently for each Procgen game to reproduce the results reported in the original paper. For a fair comparison with other methods, we use the same set of hyperparameters for all Procgen games with the best overall performance provided by the authors. More specifically, we use $E_\pi = 1$, $E_V = 9$, $N_\pi = 1$, $\alpha_a = 0.25$, and $\alpha_i = 0.001$. We also find that the performance of DAAC is better than IDAAC when using a single set of hyperparameters, as shown in Table 6. Therefore, we compare our methods with DAAC.

³<https://github.com/rraileanu/auto-drac>

⁴<https://github.com/facebookresearch/level-replay>

⁵<https://github.com/rraileanu/idaac>

Algorithm 2 Phasic Policy Gradient (PPG)

Require: Policy network π_θ , value network V_ϕ , auxiliary value head V_θ

- 1: **for** phase = 1, 2, ... **do**
- 2: Initialize buffer \mathcal{B}
- 3: **for** iter = 1, 2, ..., N_π **do** ▷ Policy phase
- 4: Sample trajectories τ using π_θ and compute value function target \hat{R}_t for each state $s_t \in \tau$
- 5: **for** epoch = 1, 2, ..., E_π **do**
- 6: Optimize policy objective $J_\pi(\theta)$ and value objective $J_V(\phi)$ with τ
- 7: **end for**
- 8: Add (s_t, \hat{R}_t) to \mathcal{B}
- 9: **end for**
- 10: **for** iter = 1, 2, ..., E_{aux} **do** ▷ Auxiliary phase
- 11: Optimize value objective $J_V(\phi)$, auxiliary objective $J_{\text{aux}}(\theta)$, and policy regularizer $C_\pi(\theta)$ with \mathcal{B}
- 12: **end for**
- 13: **end for**

Table 5: PPG-specific hyperparameters.

Hyperparameter	Value
# policy phases per auxiliary phase (N_π)	32
# policy epochs (E_π)	1
# value epochs (E_V)	1
# auxiliary epochs (E_{aux})	6
Policy regularizer coefficient (β_π)	1.0
# minibatches per auxiliary epoch per N_π	16

Table 6: PPO-normalized train and test scores of DAAC and IDAAC. Each agent is trained on 200 training levels for 25M environment steps. The mean and standard deviation are computed over 10 different runs.

	DAAC	IDAAC
PPO-norm train score (%)	104.4 ± 4.1	99.7 ± 5.4
PPO-norm test score (%)	136.7 ± 7.6	129.9 ± 7.8

DCPG We build DCPG on top of the implementation of PPG. DCPG introduces one additional hyperparameter compared to PPG, named the value regularizer coefficient. The value regularizer coefficient β_V denotes the weight for the value regularizer C_V when jointly optimized with the policy objective J_π . We use the default hyperparameter setting in Table 5 for PPG hyperparameters. We set the value regularizer coefficient to $\beta_V = 1.0$ without any hyperparameter tuning.

DDCPG We implement the discriminator for the dynamics learning using a fully-connected layer of hidden sizes [256, 256] with ReLU activation. DDCPG introduces two additional hyperparameters compared to DCPG. First, the dynamics objective coefficient β_f denotes the weight of the dynamics objective J_f when jointly optimized with the value objective J_V and the policy regularizer C_π . We set the dynamics objective coefficient to $\beta_f = 1.0$ without any hyperparameter tuning. Second, the inverse dynamics coefficient η is the hyperparameter that controls the strength of the inverse dynamics learning relative to the forward dynamics learning. We sweep the inverse dynamics coefficient within a range of $\eta \in \{0.5, 1.0\}$ and choose $\eta = 0.5$. We use the same hyperparameter setting as DCPG for the other hyperparameters.

E More Results on Progen Benchmark

The training and test performance curves of DCPG, DDCPG, and baseline methods for all 16 Progen games are shown in Figures 11 and 12, respectively. The results of UCB-DrAC and PLR are omitted in the figures for better visibility. The average training returns of DCPG, DDCPG, and all baselines are presented in Table 7. Our methods also achieve better training performance and sample efficiency than all baselines.

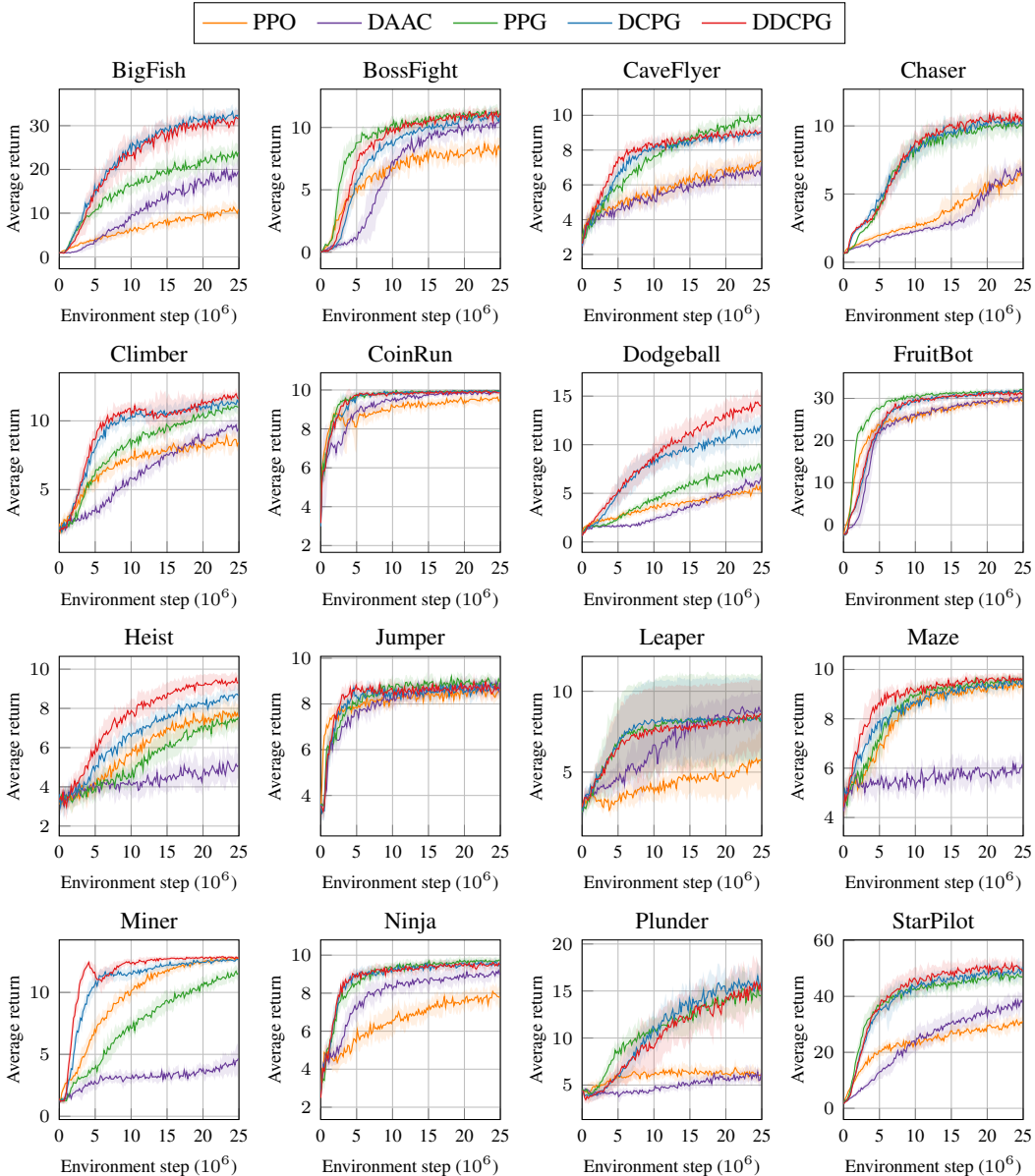


Figure 11: Training performance curves of each method on all 16 Progen games. Each agent is trained on 200 training levels for 25M environment steps and evaluated on the same training levels. The mean and standard deviation are computed over 10 different runs.

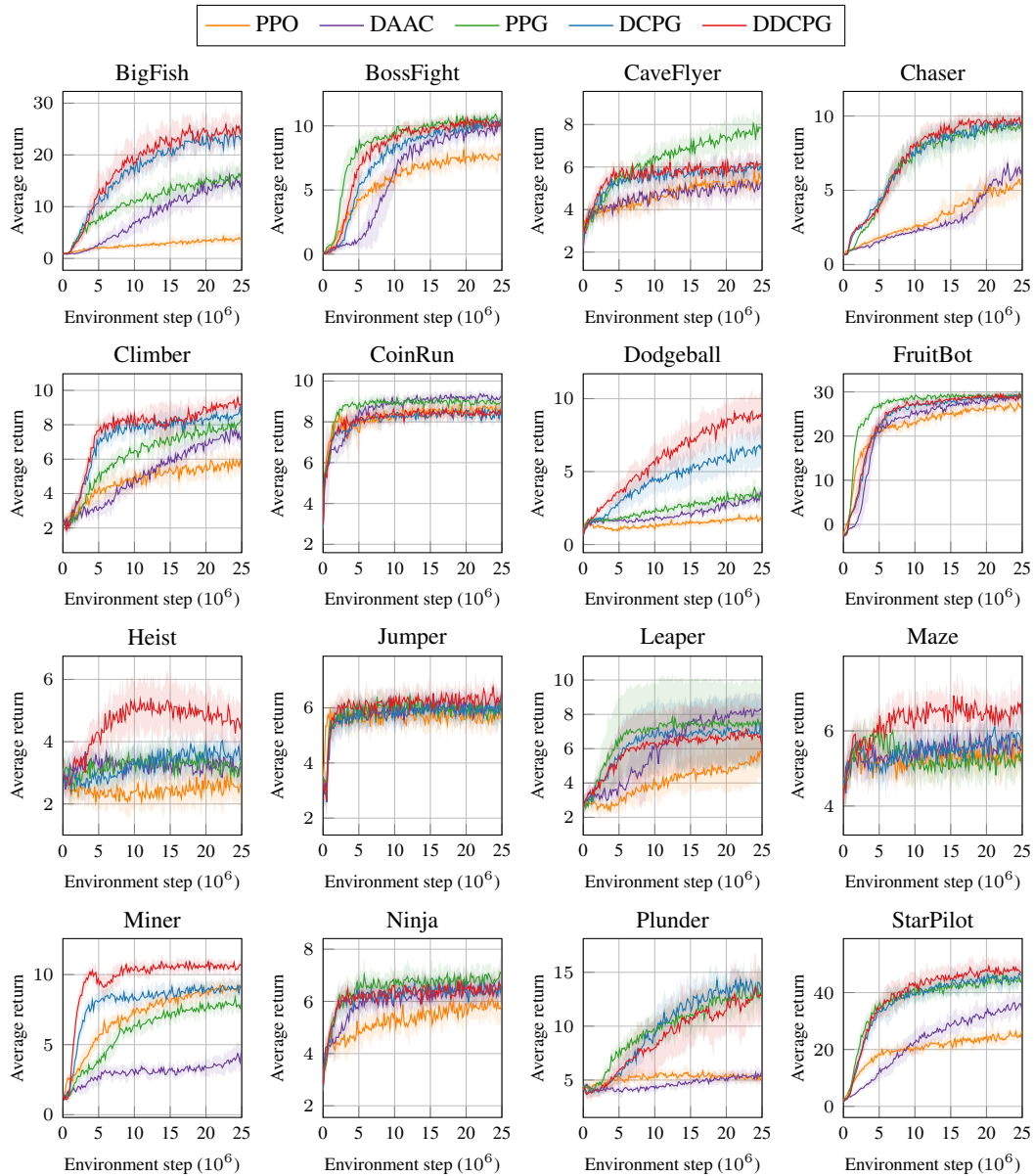


Figure 12: Test performance curves of each method on all 16 Procgen games. Each agent is trained on 200 training levels for 25M environment steps and evaluated on 100 unseen test levels. The mean and standard deviation are computed over 10 different runs.

Table 7: Average training returns of each method on all 16 Procgen games. Each agent is trained on 200 training levels for 25M environment steps and evaluated on the same training levels. The mean and standard deviation are computed over 10 different runs.

Environment	PPO	UCB-DrAC	PLR	DAAC	PPG	DCPG	DDCPG
BigFish	11.0 ± 1.7	12.2 ± 3.1	13.6 ± 3.0	18.4 ± 3.3	24.1 ± 1.6	32.8 ± 2.0	31.8 ± 2.1
BossFight	7.9 ± 0.7	8.2 ± 0.7	8.8 ± 0.7	9.9 ± 0.7	11.1 ± 0.3	10.7 ± 0.6	11.0 ± 0.5
CaveFlyer	7.1 ± 0.9	6.0 ± 0.9	7.3 ± 0.5	6.8 ± 0.8	10.0 ± 0.5	9.0 ± 0.5	9.0 ± 0.3
Chaser	6.4 ± 0.8	7.3 ± 0.7	8.0 ± 0.6	6.4 ± 1.0	10.0 ± 0.7	10.4 ± 0.6	10.6 ± 0.5
Climber	8.4 ± 0.5	8.4 ± 0.6	8.6 ± 0.6	9.3 ± 0.6	10.9 ± 0.4	11.3 ± 0.5	11.9 ± 0.4
CoinRun	9.6 ± 0.1	9.5 ± 0.2	9.4 ± 0.3	9.9 ± 0.1	10.0 ± 0.1	9.9 ± 0.1	9.9 ± 0.1
Dodgeball	5.5 ± 0.7	8.0 ± 1.2	5.1 ± 0.8	6.4 ± 0.9	7.9 ± 0.7	11.9 ± 1.4	14.1 ± 1.1
FruitBot	29.9 ± 0.5	29.1 ± 1.3	28.3 ± 1.3	29.8 ± 1.1	31.9 ± 0.4	31.9 ± 0.4	31.1 ± 0.8
Heist	7.6 ± 0.6	7.2 ± 0.6	8.0 ± 0.5	4.9 ± 0.8	7.4 ± 0.6	8.6 ± 0.4	9.4 ± 0.4
Jumper	8.7 ± 0.3	8.4 ± 0.5	8.6 ± 0.3	8.8 ± 0.3	9.1 ± 0.3	8.6 ± 0.4	8.9 ± 0.3
Leaper	5.8 ± 1.5	3.6 ± 1.1	7.0 ± 0.6	8.8 ± 1.0	8.2 ± 2.9	8.4 ± 2.3	8.4 ± 2.3
Maze	9.3 ± 0.3	8.5 ± 0.5	9.2 ± 0.4	5.7 ± 0.4	9.5 ± 0.3	9.6 ± 0.2	9.7 ± 0.2
Miner	12.8 ± 0.2	12.4 ± 0.3	11.4 ± 0.6	4.7 ± 0.7	11.6 ± 0.4	12.7 ± 0.1	12.8 ± 0.1
Ninja	7.8 ± 0.4	7.5 ± 1.0	8.2 ± 0.4	9.0 ± 0.2	9.8 ± 0.2	9.6 ± 0.1	9.6 ± 0.2
Plunder	6.2 ± 0.7	9.2 ± 1.3	11.0 ± 1.1	5.9 ± 0.6	14.5 ± 2.1	15.7 ± 1.8	16.0 ± 2.3
StarPilot	29.9 ± 3.6	30.2 ± 2.4	26.3 ± 3.2	39.0 ± 2.5	48.4 ± 3.4	50.5 ± 1.8	50.8 ± 4.0
PPO-norm score (%)	100.0 ± 2.5	102.6 ± 3.4	107.9 ± 3.5	104.4 ± 4.1	136.7 ± 4.4	148.9 ± 4.3	152.7 ± 4.4

F Ablation Studies

F.1 Delayed Critic Update

To disentangle the effect of the delayed critic update on learning generalizable representations for the policy network, we introduce a variant of DCPG that employs an additional value network V_ϕ with a separate encoder, namely Separate DCPG. The separate value network V_ϕ is trained in the same way as PPG without any delayed update and used only for policy optimization. The original value network V_θ is trained with the delayed update and used only for learning representation for the policy network.

Algorithm 3 describes the detailed procedure of Separate DCPG (differences with DCPG are marked in cyan). Note that we compute two bootstrapped value function targets $\hat{R}_{t,\theta}$ and $\hat{R}_{t,\phi}$ for each state s_t using the original value network V_θ and the separate value network V_ϕ , respectively. Each value function target is stored in a buffer \mathcal{B} and used to train the corresponding value network during the auxiliary phase.

Algorithm 3 Separate Delayed-Critic Policy Gradient (Separate DCPG)

Require: Policy network π_θ , value network V_θ , **separate value network V_ϕ**

- 1: **for** phase = 1, 2, ... **do**
- 2: Initialize buffer \mathcal{B}
- 3: **for** iter = 1, 2, ..., N_π **do** ▷ Policy phase
- 4: Sample trajectories τ using π_θ
- 5: Compute value function targets $\hat{R}_{t,\theta}$ **and** $\hat{R}_{t,\phi}$ for each state $s_t \in \tau$
- 6: **for** epoch = 1, 2, ..., E_π **do**
- 7: Optimize policy objective $J_\pi(\theta)$ and value regularizer $C_V(\theta)$ with τ
- 8: **Optimize value objective $J_V(\phi)$ with τ**
- 9: **end for**
- 10: Add $(s_t, \hat{R}_{t,\theta}, \hat{R}_{t,\phi})$ to \mathcal{B}
- 11: **end for**
- 12: **for** iter = 1, 2, ..., E_{aux} **do** ▷ Auxiliary phase
- 13: Optimize value objective $J_V(\theta)$ and policy regularizer $C_\pi(\theta)$ with \mathcal{B}
- 14: **Optimize value objective $J_V(\phi)$ with \mathcal{B}**
- 15: **end for**
- 16: **end for**

Figures 13 and 14 demonstrate the training and test performance curves of PPG, Separate DCPG, and DCPG. We find that Separate DCPG achieves better or comparable performance in most games. This implies that the value network with delayed updates can provide better representations that generalize

well to both the training and test environments than those without delayed updates. We also provide the PPO-normalized training and test scores of PPG, Separate DCPG, and DCPG in Table 8.

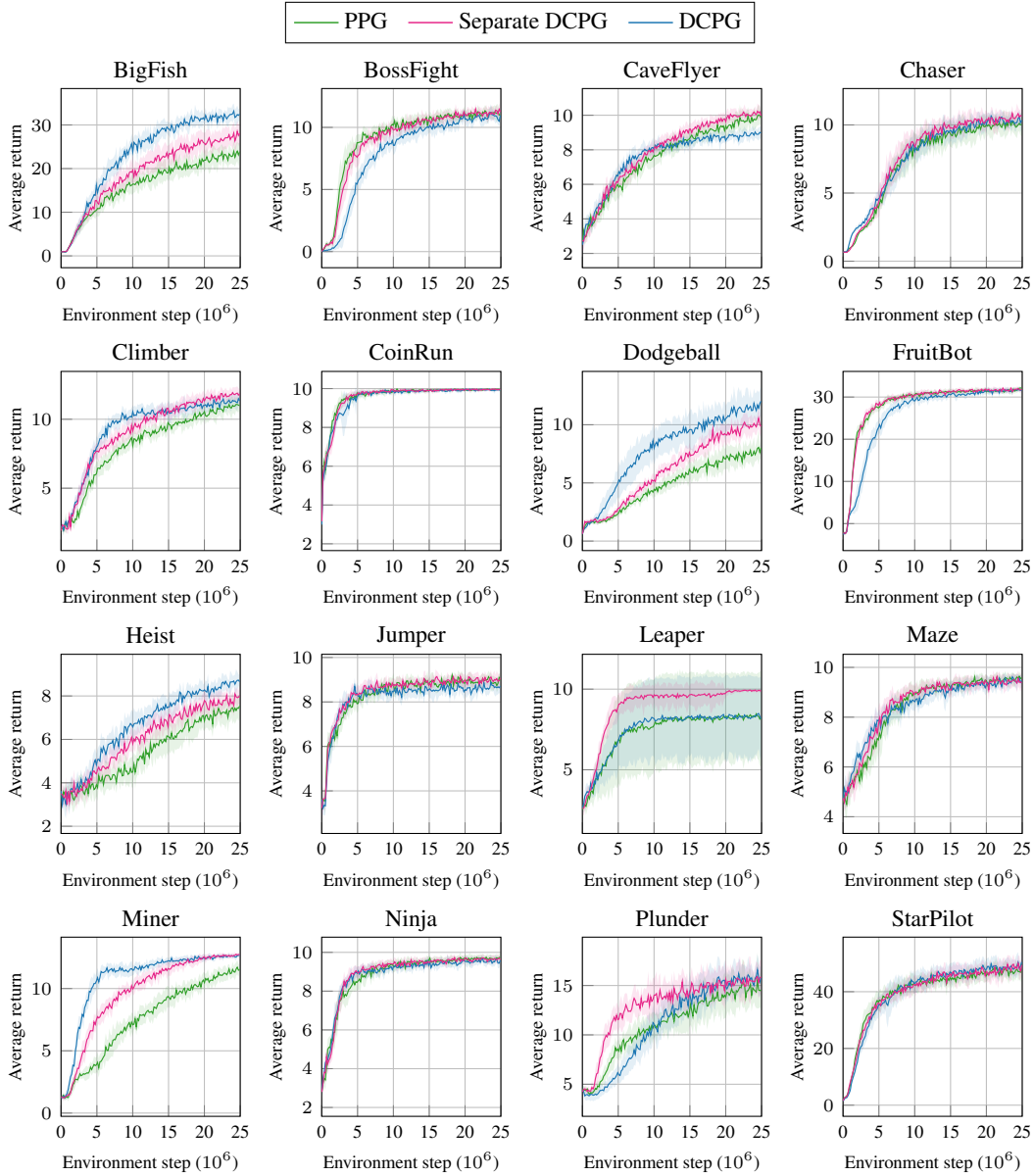


Figure 13: Training performance curves of PPG, Separate DCPG, and DCPG on all 16 procgen games. Each agent is trained on 200 training levels for 25M environment steps and evaluated on the same training levels. The mean and standard deviation are computed over 10 different runs.

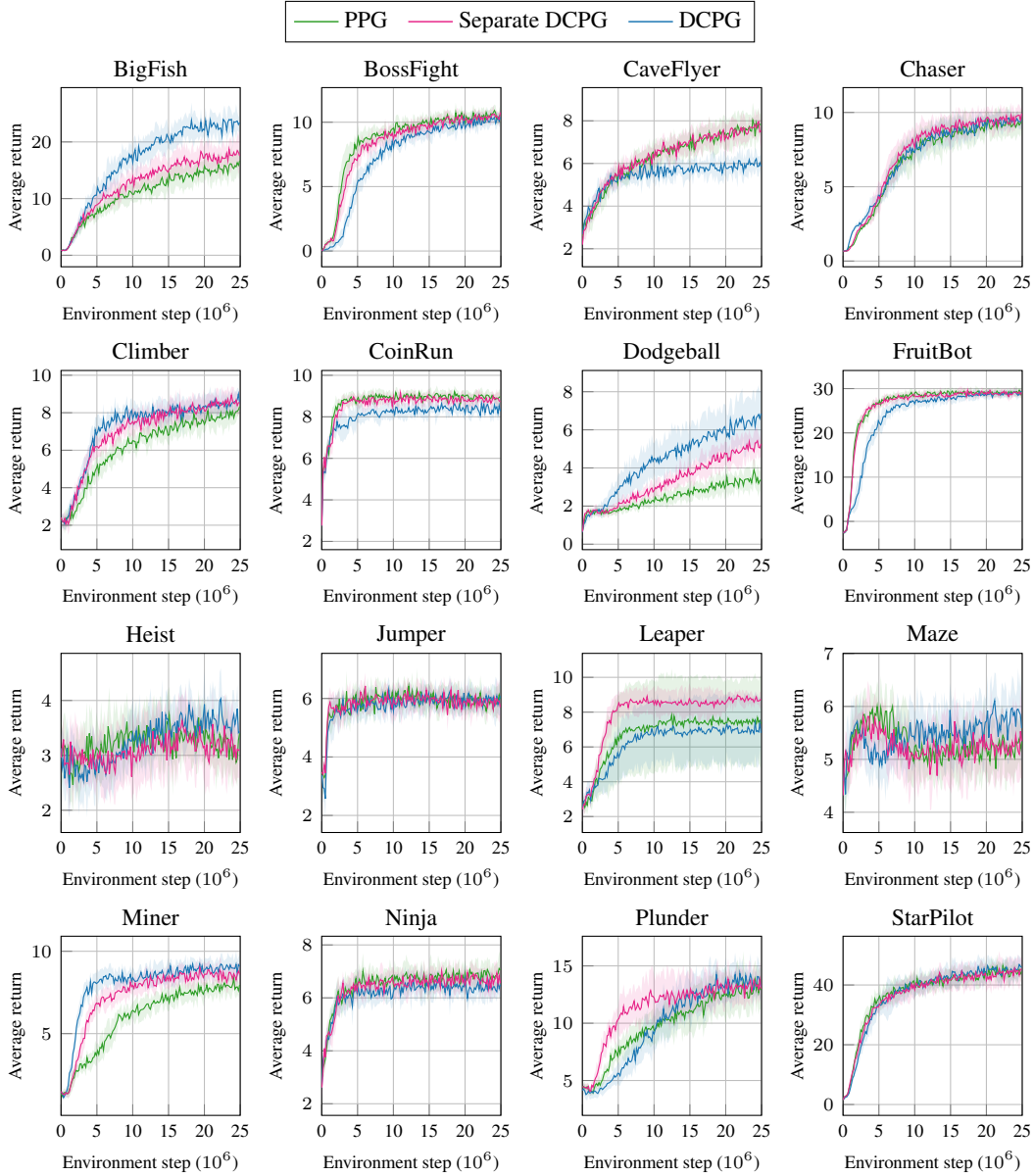


Figure 14: Test performance curves of PPG, Separate DCPG, and DCPG on all 16 procgen games. Each agent is trained on 200 training levels for 25M environment steps and evaluated on 100 unseen test levels. The mean and standard deviation are computed over 10 different runs.

Table 8: PPO-normalized training and test scores of PPG, Separate DCPG, and DCPG on all 16 Procgen games. Each agent is trained on 200 training levels for 25M environment steps. The mean and standard deviation are computed over 10 different runs.

	PPG	Separate DCPG	DCPG
PPO-norm train score (%)	136.7 ± 4.4	147.5 ± 1.9	152.7 ± 4.4
PPO-norm test score (%)	160.3 ± 6.3	174.4 ± 4.9	184.5 ± 5.2

F.2 Dynamics Learning

To demonstrate the effectiveness of learning forward and inverse dynamics with a single discriminator, we conduct experiments for DCPG with forward dynamics learning (DCPG+F), inverse dynamics learning (DCPG+I), and forward and inverse dynamics learning using two separate discriminators (DCPG+FI). The dynamics objective J_f of each algorithm is defined as follows:

$$\begin{aligned}
 J_f(\theta) &= \mathbb{E}_{s_t, a_t, s_{t+1} \sim \mathcal{B}} [\log (f_{\theta}(s_t, a_t, s_{t+1})) + \log (1 - f_{\theta}(s_t, a_t, \hat{s}_{t+1}))] && \text{(DCPG+F)} \\
 J_f(\theta) &= \mathbb{E}_{s_t, a_t, s_{t+1} \sim \mathcal{B}} [\log (f_{\theta}(s_t, a_t, s_{t+1})) + \log (1 - f_{\theta}(s_t, \hat{a}_t, s_{t+1}))] && \text{(DCPG+I)} \\
 J_f(\theta) &= \mathbb{E}_{s_t, a_t, s_{t+1} \sim \mathcal{B}} [\log (f_{\theta}(s_t, a_t, s_{t+1})) + \log (1 - f_{\theta}(s_t, a_t, \hat{s}_{t+1}))] \\
 &\quad + \eta \mathbb{E}_{s_t, a_t, s_{t+1} \sim \mathcal{B}} \left[\log \left(\tilde{f}_{\theta}(s_t, a_t, s_{t+1}) \right) + \log \left(1 - \tilde{f}_{\theta}(s_t, \hat{a}_t, s_{t+1}) \right) \right]. && \text{(DCPG+FI)}
 \end{aligned}$$

Note that we use an additional discriminator \tilde{f} for inverse dynamics in DCPG+FI. For each algorithm, we train agents using 200 training levels for 25M environment steps on 16 Procgen games. We set the dynamics objective coefficient to $\beta_f = 1.0$ without any hyperparameter tuning. For DCPG+FI, we sweep the inverse dynamics coefficient within a range of $\eta \in \{0.5, 1.0\}$ and choose $\eta = 1.0$. Table 9 shows the PPO-normalized training and test scores of each algorithm.

Table 9: PPO-normalized training and test scores of DCPG and DCPG with dynamics learning on all 16 Procgen games. Each agent is trained on 200 training levels for 25M environment steps. The mean and standard deviation are computed over 10 different runs.

	DCPG	DCPG+F	DCPG+I	DCPG+FI	DDCPG
PPO-norm train score (%)	148.9 ± 4.3	150.6 ± 3.1	149.1 ± 3.4	150.5 ± 2.5	152.7 ± 4.4
PPO-norm test score (%)	184.5 ± 5.2	195.9 ± 7.7	185.5 ± 6.5	194.6 ± 6.2	202.2 ± 10.2

Our intuition of jointly learning forward and inverse dynamics using a single discriminator is that naively learning the forward dynamics will discard the action’s information and capture only the proximity of two consecutive states in the latent space, not the dynamics. Also, additional training of the inverse dynamics with a separate discriminator cannot completely resolve this problem.

To validate this, we train three types of DCPG agents with dynamics learning, DCPG+F, DCPG+FI, and DDCPG on BigFish and count the number of OOD actions that the forward dynamics discriminator determines to be valid given a transition (s_t, a_t, s_{t+1}) from the training environments, *i.e.*, $\sum_{\hat{a}_t \neq a_t} \mathbb{1}[f(s_t, \hat{a}_t, s_{t+1}) > 0.5]$. Note that there are 9 different actions (8 directional moves and 1 do nothing) in BigFish. Table 10 shows that the discriminators of DCPG+F and DCPG+FI determine multiple OOD actions to be valid, which implies that it does not fully utilize the action information and fail to learn the dynamics.

Table 10: The number of OOD actions classified as valid for DCPG+F, DCPG+FI, and DDCPG on Bigfish. Each agent is trained on 200 training levels for 25M environment steps.

	DCPG+F	DCPG+FI	DDCPG
# OOD actions (↓)	7.05 ± 1.47	2.49 ± 1.38	0.74 ± 0.75

Furthermore, we train PPG agents with our proposed dynamics learning (named DPPG) to check whether the effect of the delayed critic update and the dynamics learning are complementary. Table 11 shows that dynamics learning is also helpful to PPG, while the extent of performance improvement is smaller than DCPG. It implies that the effects of the delayed value update and the dynamics learning are synergistic.

Table 11: PPO-normalized test scores of PPG, DPPG, DCPG, and DDCPG on all 16 Procgen games. Each agent is trained on 200 training levels for 25M environment steps. The mean and standard deviation are computed over 10 different runs.

	PPG	DPPG	DCPG	DDCPG
PPO-norm score (%)	160.3 ± 6.3	171.7 ± 4.9	184.5 ± 5.2	202.2 ± 10.2

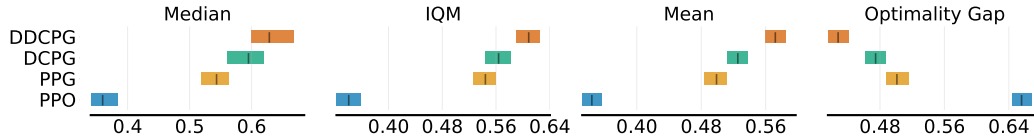


Figure 15: Median/IQM/Mean of Min-Max normalized scores with 95% confidence intervals for PPO, PPG, DCPG, and DDCPG on all 16 Progen games. Each statistic is computed over 10 seeds.

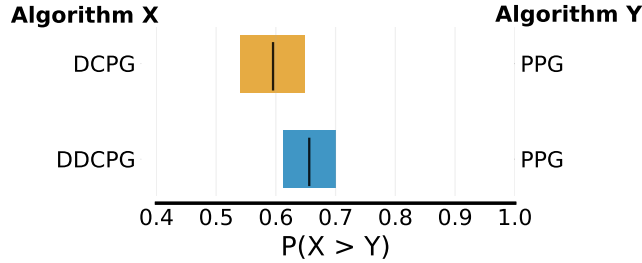


Figure 16: Probability of improvement of DCPG and DDCPG compared to PPG on all 16 Progen games. Each statistic is computed over 10 seeds.

G Evaluation using RLiabLe [2]

We also evaluated our experimental results by normalizing the average returns based on the possible minimum and maximum scores for each game and analyzing the min-max normalized scores using the RLiabLe library⁶. Figure 15 reports the Median, IQM, and Mean scores of PPO, PPG, and our methods, showing that the performance improvements of our methods are statistically significant in terms of all evaluation metrics. Figure 16 describes the probability of improvement plots comparing our methods to PPG, showing that our methods are likely to improve upon PPG.

⁶<https://github.com/google-research/rliable>